Int. J. Heat Mass Transfer. Vol. 9, pp. 739–754. Pergamon Press 1966. Printed in Great Britain

THERMAL RESISTANCES OF SOME MULTILAYER CONTACTS UNDER STATIC LOADS

T. R. THOMAS and S. D. PROBERT
School of Engineering, University College, Swansea

(*Received* 16 *November* 1965 *and in revised form* 14 *February* 1966)

Abstract—In an attempt to produce a mechanically strong thermal insulator for use at cryogenic temperatures, the variations with applied load of the thermal conductances of stacks of thin layers of stainless steel, tool steel, razor-blade steel, phenolic laminate and brass were measured *in vacuo* at room and liquid nitrogen temperatures. Each conductance is shown to consist of two components, one a constant due to radial heat leaks by conduction and radiation, the other proportional to the load raised to a power between 0·5 and 1. The latter component is found to vary inversely as the number of interfaces, and is discussed briefly from the point of view of existing theories. The mechanical and thermal properties of multilayer columns are shown to compare well with those of existing insulators, though some possible drawbacks are discussed.

NOMENCLATURE

A, area;
C, contact conductance per unit area;
D, specimen diameter;
d, strip width;
E, Young's modulus;
h, thickness of specimen layers;
K, equivalent thermal conductivity;
k, bulk thermal conductivity;
L, free height of stack;
M, Meyer hardness;
m, exponent of P in conductance equation;
N, number of layers in specimen stack;
n, number of asperities per unit area;
P, load per unit area;
p, gas pressure;
$\dot{Q}$, heat flux;
R, radius of curvature of disk;
T, absolute temperature;
Y, yield strength;
z, distance perpendicular to plane of contact;
ε, emissivity;
λ, gas mean free path;
σ, Stefan–Boltzmann constant.

Subscripts

0, zero load;
G, gas;
R, radiation;
S, solid;
T, total.

INTRODUCTION

THE THERMAL contact resistance of an interface between two solids has been the subject of a number of recent investigations, mainly from the point of view of maximizing heat transfer, as in nuclear fuel elements, aircraft and satellite joints, annealing rolled steel, etc. The literature has been reviewed extensively in references [1] and [2]. The present work involves an approach from a different angle, that of cryogenic thermal insulation.

In recent years several low temperature insulating systems of very high efficiency (the so-called "superinsulations") have been developed, but all suffer from the disadvantage of low mechanical strength. A comparatively small compressive load can irreversibly reduce the effective thermal resistivity of such materials by a factor of up to 100 [3], with possibly disastrous results to the insulated systems. The phenomenon of thermal contact resistance offers a possible solution to the problem; the elastic modulus of a number of plane interfaces in series is between

1 per cent and 10 per cent of a solid piece of the same material [4]. The insulating properties would depend on the thermal resistance of each interface and the number of interfaces.

The present investigation was an attempt to maximize the thermal resistance per unit length (equivalent thermal resistivity) due to each of these factors, to discover any interference between the two factors and to observe the variation of resistance with applied load at room and cryogenic temperatures. The amount of previous data on multiple thermal contacts is very limited. Measurement of the series thermal resistance of up to 20 interfaces between stainless steel and liquid sodium has been attempted without finding a measurable resistance [5]; the resistances of copper–steel–steel–copper and copper–nicral–nicral–copper series of interfaces have also been measured [6] and a dependence of resistance on thickness of individual layers observed. The work most closely bearing on the present problem is that of Mikesell and Scott [7], who performed measurements on columns of metal disks at cryogenic temperatures. They concluded that such systems offered considerable promise as thermal insulators, having equivalent conductivities of as low as 2 per cent that of the bulk material. They also observed that the equivalent thermal resistivity varied approximately as the inverse square root of the individual plate thickness, a result which was felt to need verification if applied to other materials. They did not investigate the effect of variation of surface properties, nor attempt a theoretical analysis of their results.

EXPERIMENTAL WORK

Mikesell and Scott found that the thermal resistance of N contacts in series was proportional to N. As this is not really self-evident (and is untrue for "superinsulations"), it was felt that the present experimental work should begin by checking this result, as ultimately all other conclusions depend on the relation of the total resistance to N. Thin stainless steel disks were used for these measurements. Also of great practical importance was the dependence of the solid conductance per unit area of a single interface C_S on individual layer thickness h. Ideally all the other specimen parameters should have been kept constant for this investigation, and with this end in view four sheets of brass shimstock of different thickness from the same source were used. (Table 1 shows that these conditions were fulfilled fairly well for the number of asperities per unit area n and the surface hardness M, though the surface roughness was high for the 0·058 mm specimen). However, with the limited resources available, it proved difficult to separate the effects of surface hardness and bulk thermal conductivity k_S. The specimens finally chosen were of tool steel (of low k_S and high M), razor-blade steel (of low k_S and very high M) and laminated resin (of very low k_S and M). Finally, the variation of thermal conductance of four of the specimens was investigated at liquid nitrogen temperatures.

Specimens

The specimens used were obtained from the following sources: Firth Vickers "Staybrite" F.S.T. stainless steel, Firth Brown "Speedicut 14" tool steel, Tufnol "Carp" fabric laminated phenolic resin, "Ever Ready" stainless steel razor-blade blanks and Macready's Metals shimstock brass.

The Staybrite stainless steel specimens and brass specimens were assembled from 1·9 cm diameter disks cut from sheet with a special punch. Slight curvature was produced by the punch in many of the disks, the effect of which was minimized by assembling the layers at random.

The tool steel disks were supplied cut to 1·9 cm diameter by the manufacturer.

The razor-blade blanks supplied by the manufacturer were cut to shape but with edges not ground. The property of particular interest was their very high hardness. As this was only imparted after the sheet had been cut into blanks it was necessary to use their peculiar form.

The laminated resin specimens were assembled

from squares cut with a guillotine, as the punch was found to damage this sheet.

Full details of specimen properties are given in Table 1.

Measurement of surface properties

Measurements of surface hardness were made on all specimens (except the phenolic laminate) using a Vickers micro-indenter and projection microscope. Satisfactory impressions could not be obtained with the laminate material, and the value quoted is converted from the manufacturer's Rockwell number. For each specimen several measurements were made on each side of a single disk or rectangle. This was repeated for several similar areas and the overall arithmetic mean taken. Measurements are given as values of Meyer hardness M (i.e. the ratio of load to projected area of indentation)—see Table 1.

Surface roughness and the wavelength of microscopic asperities were measured with a Talysurf profilometer (Rank Taylor Hobson Ltd.). The centre-line-average roughness was read off the instrument's electronic integrating meter and a chart recording of the actual surface profile was obtained simultaneously. The average wavelength of the microscopic asperities was found by counting the number of peaks per unit length of surface on the chart recording. A number of layers of each material were examined, and each was measured in two mutually perpendicular directions on either side. From these figures a CLA value for roughness and a mean number of asperities per unit area, n, were calculated for each specimen (see Table 1). The maximum wavelength cut-off in the Talysurf instrument is 0·8 mm as normally used. It is thus impossible to register waviness if its wavelength exceeds this figure. To investigate the presence of waviness the specimen under measurement was held against a steel block of surface-plate finish by two steel straps in order to remove buckle. A reference stylus then moved over an optical flat as a datum while the profilometer needle moved over the specimen and the difference in levels between the specimen and the flat was recorded on the chart. No real evidence of waviness was found for any of the specimens, though residual buckle was present in several.

Two comments on the measurements must be

Table 1. Properties of specimens at 293°K.

Material	Composition (%)	k_S (W cm^{-1} degK^{-1})	h (mm)	M (kg mm^{-2})	R (cm)	n (cm^{-2})	CLA roughness (10^{-4} cm)
Staybrite F.S.T.	C 0·07, Si 0·6, Mn 0·8, Cr 18, Ni 9	0·15	0·056	320	106	4750	0·37
Speedicut 14	C 0·6, Cr 3·5, V 0·65, W 14	0·10	0·672	496	360	2460	0·65
Carp	fabric laminated phenolic resin	0·0035*	0·178	39 to 44	76	28·4	0·43
Ever Ready blade blanks	C 1, Cr 12–13, Mn 1, Si 0·1, P 0·02, S 0·01	0·23	0·108	820	—	6900	0·062
Brass	Cu 70, Zn 30	0·96	0·413	214	95	3000	0·21
			0·282	203	60	3290	1·18
			0·140	182	156	3300	0·25
			0·058	145	143	3440	0·48

* Perpendicular to plane of sheet.

made. Firstly, due to the shape of the razor-blade blanks, no profiles could be obtained in a transverse direction, and the figures given are averages in the longitudinal direction only for both sides. Secondly, the extremely low value of n for the laminate specimens was self-consistent: no smaller asperities were observed even at the limits of magnification (50000× vertical, 100× horizontal).

Measurements of the radius of curvature (R) were by indirect means. The free height L of a column of N disks of diameter D was measured. Simple geometry then gives

$$R = \frac{D^2}{8(L/N - h)} \quad (1)$$

In the case of the laminate specimens, D was taken as the length of the diagonal. No such measurements were attempted for the razor-blade blanks. The measured values of R (see Table 1) are, of course, average, and do not imply that particular disks were spherically curved.

DESCRIPTION OF APPARATUS

The thermal conductance apparatus (see Fig. 1) has been described in detail elsewhere [8] and only a brief account of it will be given here. The heat sink was a hollow copper cylinder which could be filled with liquids or liquefied gases appropriate to the temperature range under consideration. A hollow tube passed through the heat sink and contained a shaft through which load was transmitted to the specimen assembly which was supported by an adjustable platform suspended from the base of the heat sink. Specimen chamber and heat sink were enclosed in a copper vacuum jacket, and the whole apparatus surrounded by a Dewar flask containing the appropriate liquid for stabilizing the thermal environment. The temperature of the heat sink could be varied by reducing the pressure above the boiling liquid it contained. To this end, it was connected to a rotary vacuum pump and a manostat. The tube containing the load-bearing shaft served also as the sink-fluid pumping line, and for this reason stainless steel bellows were used at its upper and lower extremities to allow vertical movement of the shaft while preserving vacuum integrity. Load was applied to the shaft by a lever and hanging weights arrangement (see Fig. 1): this "dead-weight" method has the advantage of maintaining a constant load despite thermal changes in specimen geometry.

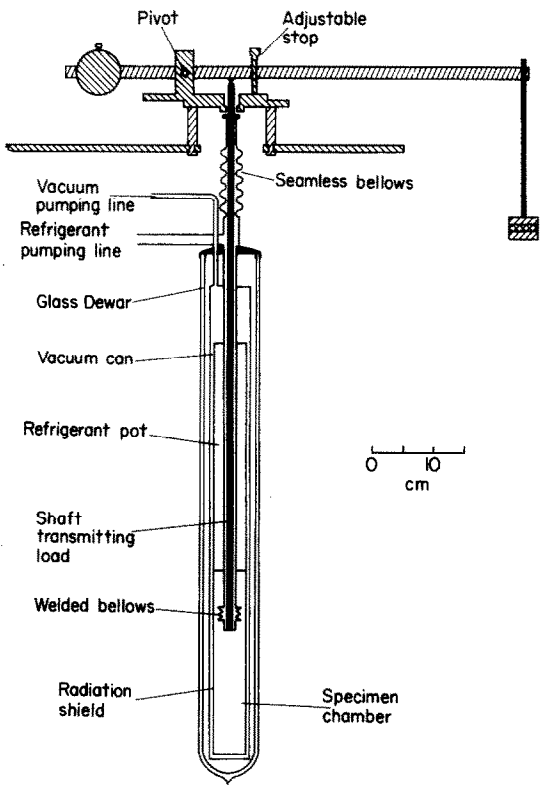

FIG. 1. Thermal conductance apparatus.

Two specimens of each material were used in each measurement with a heater between them (see Fig. 2). The specimens contained the same number of interfaces and it was assumed that their behaviour under load was identical. If a single specimen had been used, as in a normal thermal conductivity apparatus, the stray heat leak through the heater support would have been of the same order of magnitude as the heat flux through the specimen. The heater used was a 100 kΩ wire potentiometer track embedded in

a copper block, and power was supplied to it at up to 80 V from a specially developed circuit [9]. Thus the necessary current was very small and the heat leak could be minimized by using very fine leads.

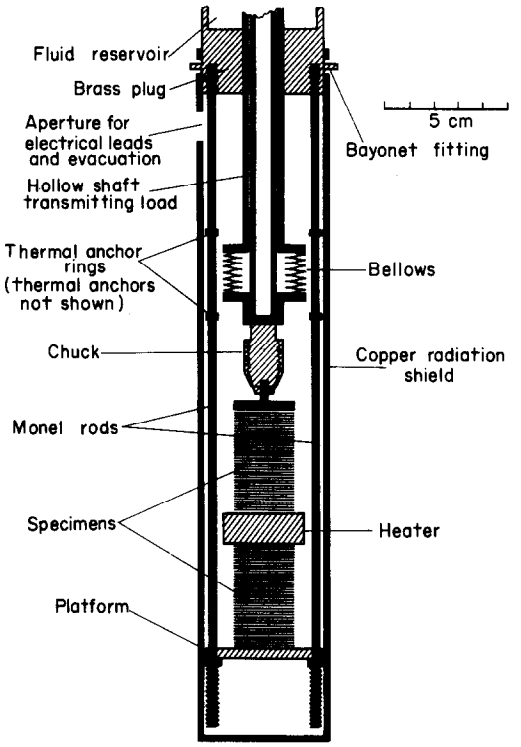

FIG. 2. Specimen chamber.

The resistance of the heater was initially measured with a Wheatstone bridge at room temperature and 77°K. The heater current was determined by balancing the potential drop across a standard resistor in series, and hence the power dissipated in the heater was deduced. The e.m.f.s of the copper–constantan differential thermocouples used for thermometry were balanced to 10^{-7} V with a Diesselhorst potentiometer having thermoelectric-free accessories. Stray thermal e.m.f.s were backed off initially by a compensator.

Experimental procedure

Specimen lengths varied from 2 to 7 cm according to the number of layers available. Once a specimen was in position on the apparatus, constantan heater leads and thermocouple wires were attached. For the disk specimens, special brass end-plates with "horns" were made to carry the thermocouples, which were wound on the horns over a thin layer of lacquer for electrical insulation. With the phenolic laminate specimen, end plates of laminate were used and of course needed no electrical insulation. The thermocouples for the razor-blade stacks were attached directly to the platform and heaters. All electrical leads were 40 S.W.G. and spirally coiled to decrease heat leaks. The radiation shield was assembled, the vacuum can Woods-metalled in position and the vacuum system exhausted to between 10^{-3} and 10^{-4} torr.

For room temperature measurements the heat sink was filled with acetone through the siphon. (It was necessary to use a volatile liquid for ease of subsequent removal by pumping.) The vacuum flask was raised round the apparatus and filled with water: the specimen heater was switched on and adjusted to produce a temperature drop of up to 3 degK across each specimen. Twenty-four hours were allowed for the system to attain the steady state before taking measurements. After a change in applied load, it required from 6 to 12 h to restore equilibrium. Measurements were usually made at the rate of two a day.

At liquid nitrogen temperatures the procedure was somewhat different. Both the vacuum jacket and refrigerant system were exhausted initially. The outside was first cooled by slowly raising the Dewar flask filled with liquid nitrogen. Helium exchange gas was then admitted to the vacuum system to precool the heat sink, and finally the exchange gas was pumped away and liquid nitrogen siphoned into the heat sink. Relaxation times to attain the steady state at liquid nitrogen temperatures were from $1\frac{1}{2}$ to 3 h.

In the case of the tool steel and the razor-blade steel specimens at room temperature the initial load was a low weight in order to retain the specimen in position, and the initial increase

of pressure was the first to which these specimens had been subjected. In all the other runs the maximum pressure was applied to the specimens for 24 h before measurements began, in order to ensure a fully elastic response.

For the electrical resistance measurements the ends of the specimens were electrically insulated from the rest of the apparatus. Room temperature measurements were made with the potentiometer; those for the 77°K system were made with an Avometer. In all cases electrical measurements were made after thermal measurements in case thermal equilibrium was upset by Joule heating.

It was originally intended to make electrical measurements on the brass disks also, but when this was attempted it was found that reversal of the current produced changes of up to 100 per cent in the potential difference across the specimen. This is tentatively attributed to the rectifying action of copper oxide films on the contacts.

The thermal and electrical conductance results are plotted in Figs. 3–8.

Accuracy of measurements

Assuming the masses of the weights and the effective length of the moment arm were known accurately, the error in the applied pressure arose from two sources: errors in measuring specimen cross-sectional areas, and elastic reaction in the bellows. The first of these was a systematic error in any one run and did not affect the relative accuracy of results in that run. It might have amounted to as much as 10 per cent in the case of the disks and rather less for the others. The error due to the bellows varied with the applied load. Attempts to measure it by using a germanium crystal in place of the specimen as a strain gauge were unsuccessful. Rough measure-

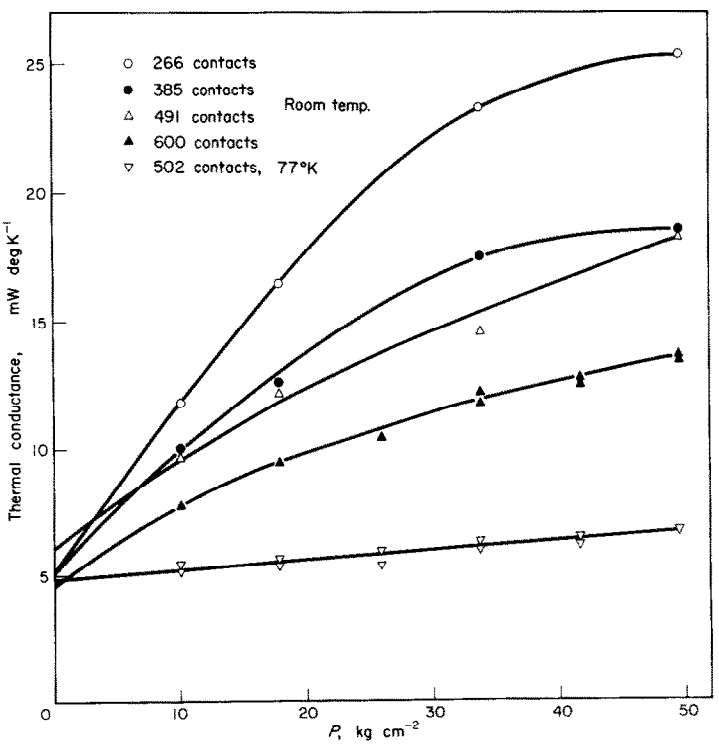

FIG. 3. Stainless steel, total conductance.

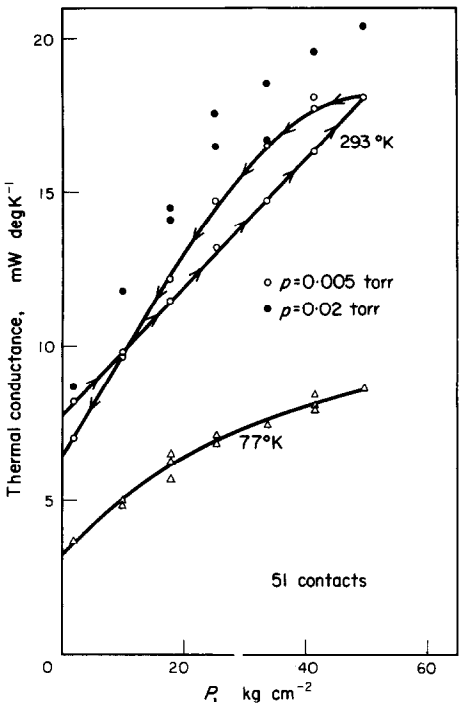

FIG. 4. Tool steel, total conductance.

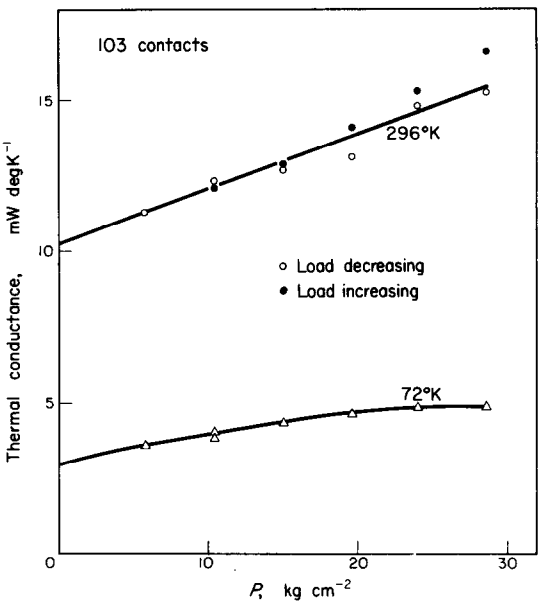

FIG. 6. Phenolic laminate, total conductance.

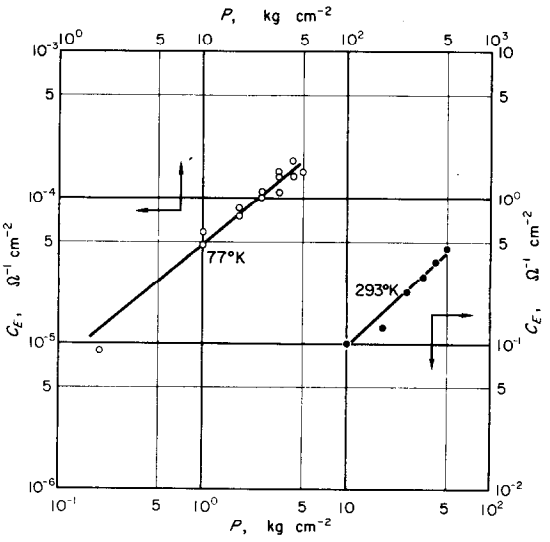

FIG. 5. Tool steel, electrical conductance.

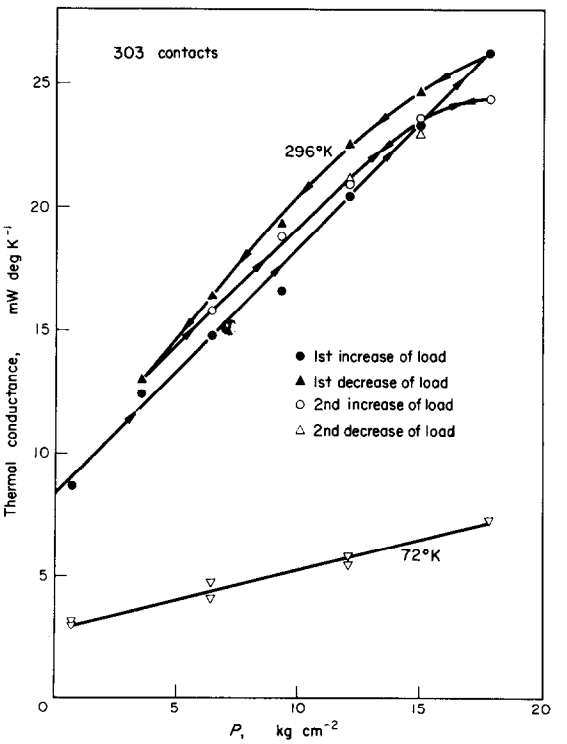

FIG. 7. Razor-blade steel, total conductance.

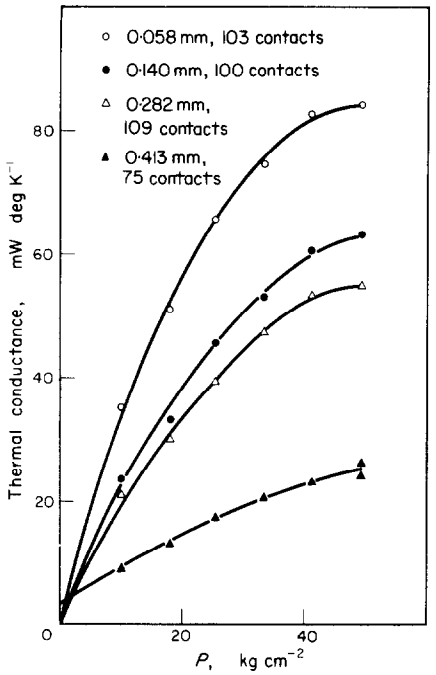

FIG. 8. Brass, total conductance.

ments at room temperature suggested that a force of about 5 kg was required to compress the bellows fully, but of course the elastic force would have been larger at low temperatures. In fact loading was always conducted so that the bellows were at medial extension after the initial load; thereafter the extension was of the order of 0·1 mm.

Errors in the thermal conductance measurements were simply those in the electrical measuring instruments. Heater power dissipations were determined to better than $\pm 0{\cdot}5\%$ absolutely and to better than $\pm 0{\cdot}1\%$ relatively. Temperature differences were measurable to $\pm 3\%$ or better in the worst cases at low temperatures, and to better than $\pm 1\%$ at room temperature. Electrical conductance measurements were accurate to $\pm 5\%$ or better at 77°K and to $\pm 0{\cdot}1\%$ at room temperature.

DISCUSSION OF RESULTS

Components of total thermal conductance

The measurements actually made in the thermal conductance experiments were those of temperature difference across the specimens and total heat input. It is now necessary to consider the various paths between the heat source and sink which this energy could have taken. The possible paths in parallel through the specimen include conduction and radiation through the interfacial fluid. Also there are the possibilities of radial convection, conduction and radiation, besides conduction through the electrical leads.

The total solid conduction through the specimen, $(C_S)_T$, can be split into two series components due to the constriction conduction across interfaces and conduction through the bulk material, i.e. for the ith layer,

$$\frac{1}{(C_S)_T} = \sum_{i=0}^{N} \left(\frac{1}{C_S A}\right)_i + \sum_{i=0}^{N+1} \left(\frac{h}{k_S A}\right)_i \quad (2)$$

Approximate values of C_S can be predicted from reference [1]. If these are compared with the values of k_S and h in Table 1, it can be seen that the second term of equation (2) is unlikely to exceed 10 per cent of the first, and will in most cases be of the order of 1 per cent. We may then write as a fair approximation

$$(C_S)_T = C_S A/N. \quad (3)$$

Convection in the interfacial fluid, or between the specimen and walls of the chamber, need not be considered at these low gas pressures as the Grashof number is less than 2000 [10]. Due to the smallness of the interfacial gap and the long mean free path of the gas molecules, fluid conduction at these pressures should be free-molecular and therefore negligible compared with solid conduction (see below). There is strong experimental support for this from references [11] and [12]. In each case a sharp fall in contact conductance to a constant value was reported as the gas pressure decreased. Skipper and Wootton [11] reported this fall as being complete at 10 torr for helium at 300°C, while Shlykov and Ganin [12] found no change below 1 torr for air at about 200°C.

The maximum values of heat conductance per

unit area due to radiation across the interfacial gap (C_R) can be calculated from Stefan's law as 0·6 mW cm^{-2} degK^{-1} at room temperature and 0·01 mW cm^{-2} degK^{-1} at 77°K. These are negligible compared with the conductance results per contact obtained. It would appear, then, that in the present experiments the only heat-transfer mechanism of importance through the specimen is the solid conductance.

In the absence of other heat paths the conductance–pressure graphs would be expected to extrapolate to zero conductance at zero load. It is evident from Figs. 3, 4, 6–8, however, that they do not. The values of the intercepts C_0 vary between $\frac{1}{2}$ and 10 mW degK^{-1} (see Table 2). The explanation for this large variation must lie in the mechanisms of the radial heat leaks (those through the electrical leads can be shown to be negligible).

Convection is negligible at these vacua. To determine the part played by radiation, consider Fig. 9. One end of the specimen of length L and radius $D/2$ is at temperature T_1, the other at T_2 (where $T_1 > T_2$). Heat is lost from the sides of the specimen to the radiation shield which is at temperature T_2. If the axial temperature distribution in the specimen is assumed linear, the temperature T_Z of an element dz distant z from the sink will be

$$T_Z = T_2 + \frac{z}{L}(T_1 - T_2) \tag{4}$$

As $(T_1 - T_2) < 3$ degK, we can say that $T_1 \sim T_2 = T$ and $(T_1 - T_2) \ll T$; then from equation (30) of reference [12],

$$\mathrm{d}\dot{Q}_R = 4\pi D\, \mathrm{d}z f(\varepsilon)\sigma T^3(T_Z - T_2) \tag{5}$$

$$\dot{Q}_R = \int_0^L \frac{4\pi \mathrm{D} f(\varepsilon)\sigma T^3(T_1 - T_2)}{L} z\, \mathrm{d}z \tag{6}$$

$$= 4\pi D f(\varepsilon)\sigma T^3(T_1 - T_2)L. \tag{7}$$

For diffuse reflection between two coaxial cylinders [14],

$$f(\varepsilon) = \frac{\varepsilon_1\varepsilon_2}{\varepsilon_2 + (D_1/D_2)(1 - \varepsilon_2)\varepsilon_1} \tag{8}$$

where D_1, D_2 are the diameters of cylinders of emissivities ε_1, ε_2 respectively ($\varepsilon_2 \neq 1$).

Table 2

Material	T (°K)	Deformation	C_0 (mW °K^{-1})	m	N	Mean temp. drop (degK)
Staybrite F.S.T.	293	elastic	4·5–6·0	0·67	see Fig. 3	1·0
	77	elastic	4·8	1·0	502	2·9
Speedicut 14	293	plastic	7·7	1·0		1·8
	293	elastic	6·2	0·87	51	1·8
	77	elastic	3·1	0·74		2·3
Carp	296	elastic	10·2	1·0	103	1·3
	72	elastic	2·9	0·72		2·4
Ever Ready blade blanks	296	plastic	8·3	1·0		1·6
	296	elastic	8·3	0·82	303	1·6
	72	elastic	2·8	1·0		3·0
Brass 0·413 mm	296	elastic	3·5	0·88	75	1·4
Brass 0·282 mm	295	elastic	0·5	0·65	109	0·6
Brass 0·140 mm	294	elastic	0·5	0·65	100	0·6
Brass 0·058 mm	296	elastic	0·5	0·54	103	0·4

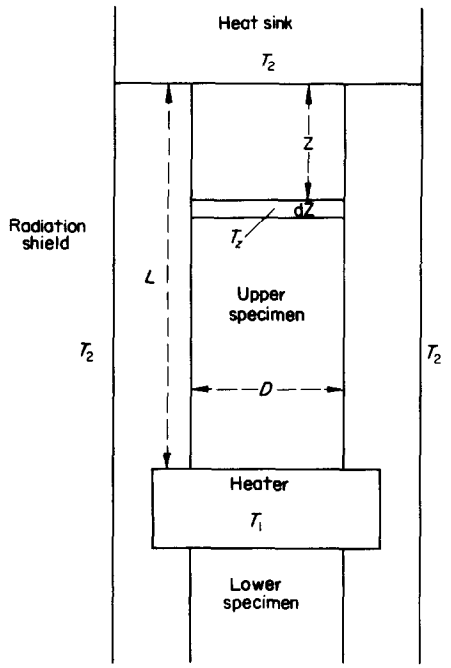

FIG. 9. Specimen chamber, showing radial heat leaks.

The emissivity of the specimen, being that of a large number of rough edges, is probably near unity. Taking the emissivity of the copper radiation shield as 0·02, then $f(\varepsilon)$ is approximately 0·06. Equation (7) then gives values of 4 mW degK^{-1} for the total radiation heat leak from the largest specimens at room temperature, assuming similar temperature distributions over each of a pair of specimens. This is too small to account for the observed variation of C_0.

There remains radial conduction through the gas. Gaseous conduction at normal pressures is independent of gas pressure, while at high vacuum it is proportional to the pressure. There is an intermediate region of pressure, known as the transition region, where conduction is by a combination of both mechanisms. The transition region is characterized by Knudsen numbers between 10 and 0·1 [15]. The Knudsen number Kd is the ratio of the molecular mean free path λ to some characteristic length, in this case the radial separation of specimen and radiation shield, which is 1·8 cm for the disk specimens.

Figure 10 shows the transition region for the two cases of present interest, air at 293°K and helium (exchange gas) at 77°K, and the calculated thermal conductances per unit area C_G for free-molecular and kinetic-theory flows. It is permissible to use interpolated conductances in the transition region [16].

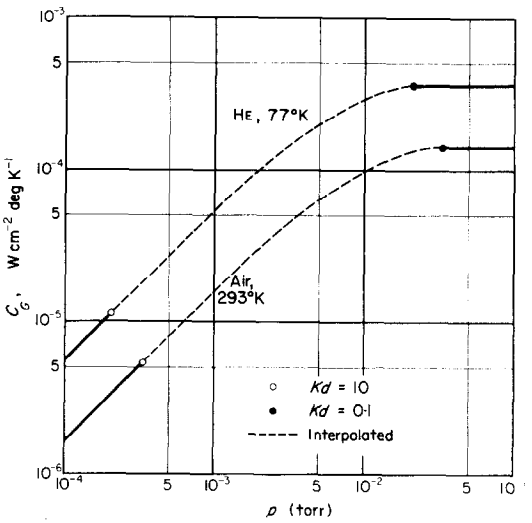

FIG. 10. Radial heat leaks through gas.

Considering again Fig. 9, the rate of heat lost by gaseous conduction from an element dz

$$d\dot{Q}_G = 2\pi D\, dz C_G(T_Z - T_2). \qquad (9)$$

From equation (4),

$$\dot{Q}_G = \int_0^L \frac{2\pi D C_G(T_1 - T_2)}{L} z\, dz \qquad (10)$$

$$\dot{Q}_G = \pi D C_G(T_1 - T_2)L/2. \qquad (11)$$

Again assuming similar temperature distributions over each of a pair of specimens, the total rate of heat lost is $2\dot{Q}_G$. As the experimental vacuum varied from experiment to experiment over the range 5×10^{-4} to 5×10^{-3} torr, it can be seen that the variations in C_G are sufficient to explain the range of values of C_0 for specimens of different sizes. Also explained is the approximately 30 per cent variation in C_0 for two different pressures for the room temperature results

of Fig. 4. C_0 is, in accordance with the above argument, invariant with the load, and so may be subtracted from all values of the total conductance to give the solid conductance.

DISCUSSION OF SOLID CONDUCTANCE DATA

Following the argument of the previous section, the intercepts C_0 were subtracted from the total conductances. The differences, the solid conductances, are plotted as conductance per contact per unit area against applied pressure in Figs. 11–15. It should be noted that in Fig. 11 there are no significant differences between the results from stacks of different numbers of contacts, i.e. the assumption of a constant conductance per contact is justified.

For surfaces in contact which conform closely on a macroscopic scale there is a well established expression for contact resistance [18]:

$$\frac{C_S'}{k_S} = \sqrt{\left(\frac{4Pn}{\pi M}\right)} \tag{12}$$

in the symbols of the present paper where C_S' is the limiting value of C_S for conforming surfaces. In the present experiments the surfaces conform most closely when, (a) the layers are most nearly flat initially, i.e. small R, (b) the layers are relatively flexible i.e. h and E are low, and (c) the applied pressure is greatest. The following values of

$$\frac{C_S}{C_S'} = \frac{C_S}{k_S}\sqrt{\left(\frac{\pi M}{4Pn}\right)}$$

were obtained at the highest applied pressures.

Staybrite	4·3
Speedicut	1·1
Carp	55
Ever Ready Blades	0·79
0·413 mm brass	0·21
0·282 mm brass	0·65
0·140 mm brass	0·64
0·058 mm brass	0·81

With two exceptions, which will be discussed first, these values are of the order expected. For the "Staybrite" the most probable explanation is that the effective value of n was greater than quoted in Table 1. For the "Carp" the value of k_S in the local phenolic material at the surface was probably very much higher than the average value of the laminate and this controls the contact conductance.

The effect of pressure on conformity and hence contact conductance can be estimated as follows. Consider two strips of material, of width d

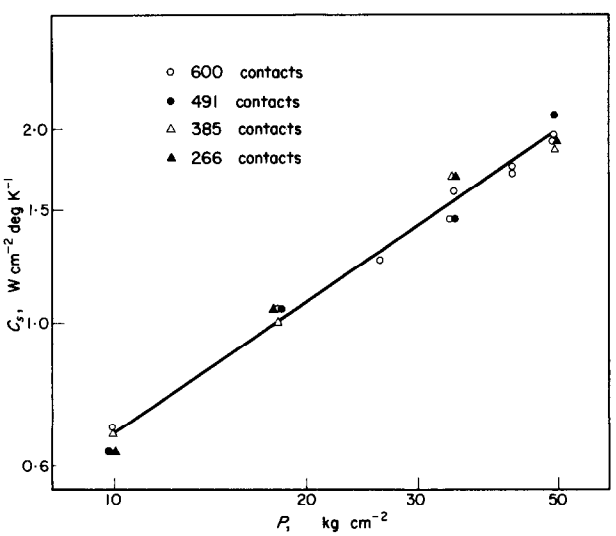

FIG. 11. Stainless steel, room temperature solid conductances.

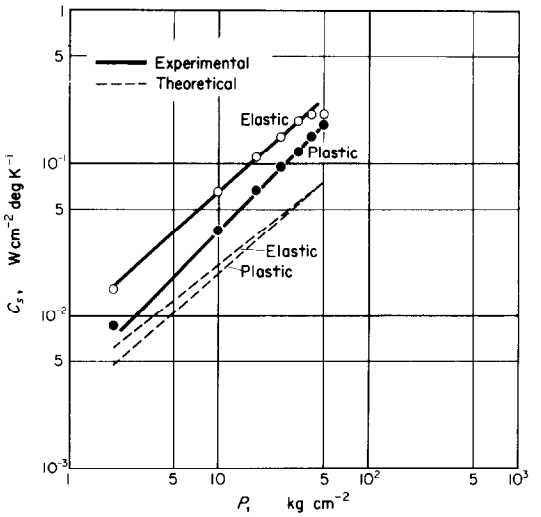

FIG. 12. Tool steel, room temperature solid conductance.

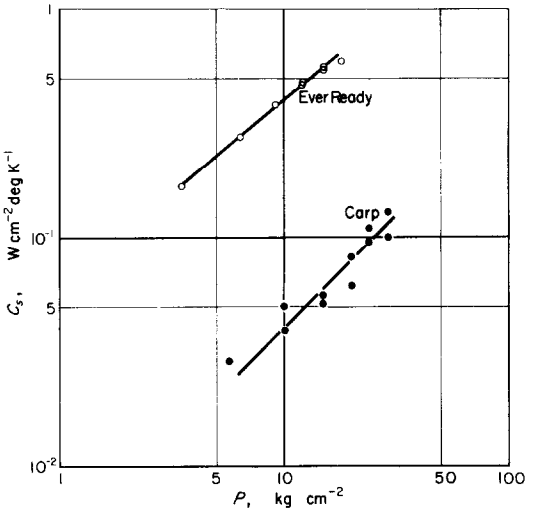

FIG. 13. Phenolic laminate and razor-blade steel, room temperature solid conductance.

and curvature R across the width, pressed together between flat anvils; the elastic theory of bending gives

$$\frac{\text{area of macroscopic contact}}{\text{area of strip}} = X \simeq 1 - \frac{Eh^3}{3PRd^2} \quad (13)$$

and

$$\frac{C_s}{C_s'} = X \sqrt{\left(\frac{\text{actual contact pressure}}{\text{apparent contact pressure}}\right)} = \sqrt{X} \quad (14)$$

Therefore

$$\left(\frac{C_s}{C_s'}\right)^2 \simeq 1 - \frac{Eh^3}{3PRd^2} \quad (15)$$

This assumes that the deflection of the layers remains elastic, and a very simple shape of initial deformation. However in general it would be expected that

$$\left(\frac{C_s}{C_s'}\right)^2 \simeq 1 - \text{constant}\,\frac{Eh^3}{PRd^2} \quad (16)$$

Qualitatively the results for various thicknesses of brass layers bear this out. It is difficult to carry the analysis much further quantitatively because the precise shape of the deformations of layers is not known. Further experimental work could establish this. The fall of C_S with reduction of P will of course be more rapid than Holm's

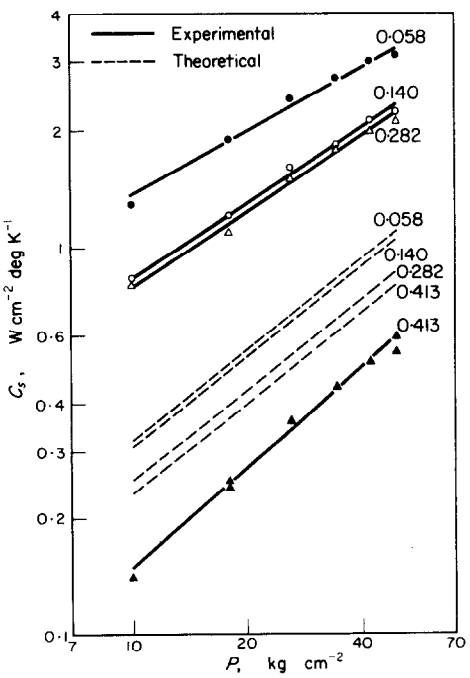

FIG. 14. Brass, room temperature solid conductance.

prediction that $C_S \propto P^m$, where $m = \frac{1}{2}$. This is confirmed by the experimental results (Table 2).

Electrical conductance results

The main purpose of the electrical conductance measurements was to observe whether similar mechanisms were operative in both electrical and thermal solid conductance. Figure 5 suggests that this is in fact the case both at room and liquid nitrogen temperatures. The slopes of the graphs are 0·93 and 0·82 respectively, compared with 0·89 and 0·74 for the corresponding thermal measurements.

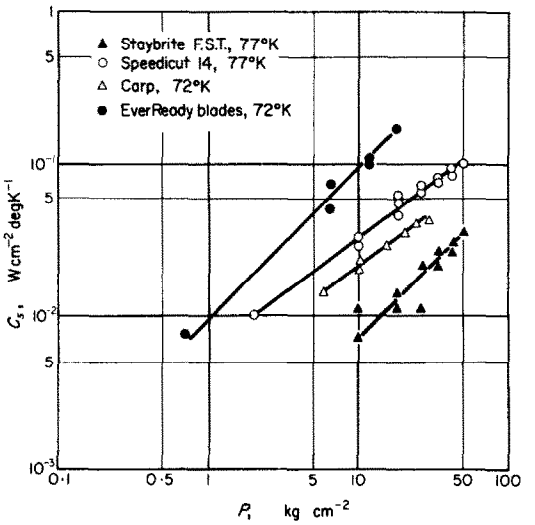

FIG. 15. Low temperature solid conductance.

The apparent Lorenz number is $\sim 10^5$ times the calculated number at 77°K, and $\sim 10^6$ times the calculated Lorenz number at room temperature. The reason for this is almost certainly the presence of an oxide film, whose thermal conductivity would be of the same order as that of the bulk material but whose electrical conductivity would be very low. No measurement of the film thickness has been attempted.

CONCLUSIONS

Application to thermal insulation

The thermal conductance per unit area per unit length, or equivalent thermal conductivity K, can be written for a long multilayer stack under vacuum conditions as K approximately equals $C_S h$. Plots of K vs. P afford a useful basis of comparison between insulations (see Fig. 16). The most promising performance, both at room and liquid nitrogen temperature, is that of the phenolic laminate.

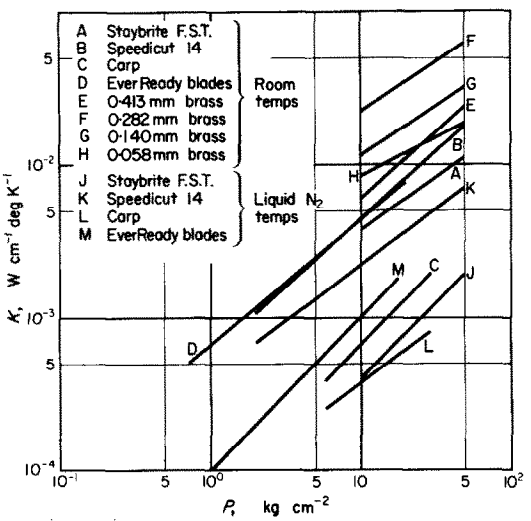

FIG. 16. Equivalent thermal conductivities.

In Table 3 the ratios of k_S to K at room temperature and $P = 10$ kg cm^{-2} are shown. These may be taken as a measure of the insulating efficiency of the stacks. If log (k_S/K_{10}) is plotted against log k_S, the points appear to be a reasonably good fit to a straight line of slope 2 (see Fig. 17), implying that K_{10} is proportional to $k_S^{\frac{1}{2}}$. No theoretical reason for this relationship is apparent, and in view of the fact that other important parameters (e.g. hardness) are not kept constant, it may be that the relation is fortuitous. If it is a real effect, however, it would indicate that little improvement in the efficiency of the insulation would result from choosing materials of lower bulk thermal conductivity.

From a practical point of view the variation of insulating efficiency with thickness of individual layers is of some importance. As the other parameters are held more or less constant in the case

Table 3

Support (multilayer unless otherwise stated)	K_{10} (mW cm^{-1} degK^{-1})	Y (kg cm^{-2})	k_S/K_{10}	Y/K_{10} (10^5 kg degK W^{-1} cm^{-1})
Staybrite F.S.T.	3·7	8200	41	22
Speedicut 14	4·4	15000	23	34
Carp	0·66	770	5·4	12
Ever Ready blade blanks	4·2	—	52	—
Brass 0·413 mm	6·0	3300	160	5·5
Brass 0·282 mm	22	3300	44	1·5
Brass 0·140 mm	11	3300	87	3·0
Brass 0·058	8·2	3300	117	4·0
Solid Dacron	1·5	1400	1	9·3
Solid Mylar	1·5	700	1	4·7
Solid* titanium alloy (4Al–4Mn)	60	10000	1	1·7

* Average value between 20°K and 300°K.

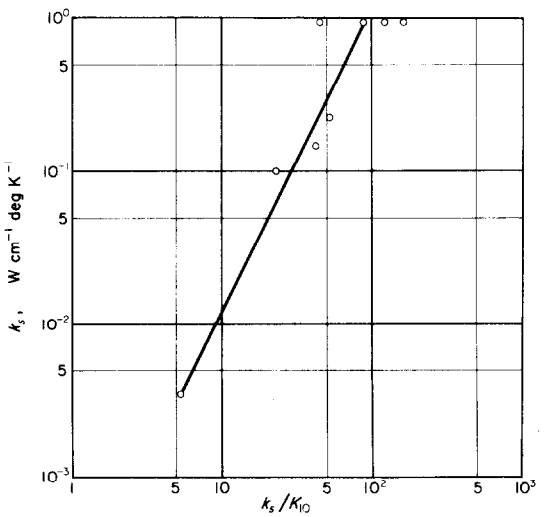

FIG. 17. Conductivity ratio vs. bulk conductivity.

of the brass specimens there is justification for plotting k_S/K_{10} vs. h for these (Fig. 18). The curve with a minimum is what would be expected from the interaction of two mechanisms, one the increase in resistance with number of contacts per unit length, the other being the increase in resistance per contact with thickness. The exact position of the minimum would presumably vary with the material, and could not be predicted without a knowledge of the variation of C_S with h. It would seem safest, in the light both of the present results and of those of Mikesell and Scott, to use the thinnest material available.

A comparison figure of merit sometimes used for cryogenic supports is the ratio of yield strength Y to thermal conductivity. The yield strengths of multilayer stacks *in compression* are those of the bulk materials. Values of Y and Y/K_{10} are shown in Table 3, together with figures for the best materials used hitherto [20].

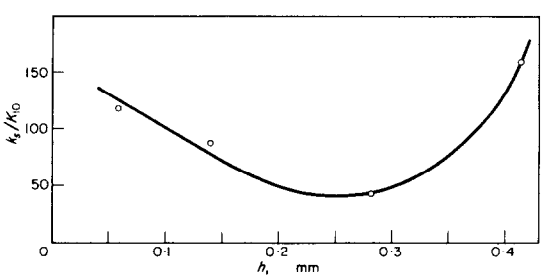

FIG. 18. Brass, conductivity ratio vs. thickness.

On this basis the use of multilayer stacks in compression appears quite promising.

One final point which should be discussed is the radiant heat exchange with an insulator of this type in practice. A realistic situation might be a stack of length 10 cm with 100 contacts per cm and boundary temperatures T_1 and T_2, being 300 and 77°K respectively. The radiative heat-transfer rate $\dot{Q}_R$ for such a system is given by Vance [3] as:

$$\frac{\dot{Q}_R}{A} = \sigma \frac{(T_1^4 - T_2^4)}{(N-1)(2-\varepsilon)} \qquad (17)$$

For $0 < \varepsilon \leqslant 1, 23 < \dot{Q}_R/A \leqslant 46\ \mu W\ cm^{-2}$. The higher figure would apply to the laminate and would be of the order of the solid conductance per unit area for P equal to 10 kg cm^{-2}.

The mechanical design of insulators embodying multilayer stacks is not within the scope of this work. It might be mentioned, however, that research on the mechanical properties of these stacks [4] has indicated that their effective elastic modulus in compression is low under small loads (where the predominant process is flattening of the buckle of the individual disks), but approaches that of the bulk material as the load is increased.

The above discussion suggests general principles for the design of insulation supports, for a given P, and overall length.

(i) k_S should be small.
(ii) n should be small, i.e. surfaces roughened.
(iii) M should be large, i.e. hard materials used.
(iv) The individual layers should be corrugated and stiff, i.e. E and h should be large.
(v) A large number of layers should be used, this will conflict with requirement (iv).

ACKNOWLEDGEMENTS

The authors are indebted to Mr. A. C. Rapier, U.K.A.E.A. Windscale, for suggesting the theoretical interpretation of the solid conductance data.

Gratitude is expressed to Messrs. Ever-Ready Razor Products and Messrs. Tufnol Limited for their provision of specimens and technical information.

This paper is published with the permission of the Managing Director of the Reactor Group of the United Kingdom Atomic Energy Authority to whom we are indebted for financial assistance. We are also grateful to the Science Research Council for supporting this project.

REFERENCES

1. T. R. Thomas and S. D. Probert, Thermal resistance of pressed contacts, UKAEA Report, TRG 1013 (R/X) (1965).
2. H. Y. Wong, Thermal conductance of metallic contacts—a survey, Paper presented at NPL Thermal Conductivity Conference, London (1964).
3. R. W. Vance, *Cryogenic Technology*, pp. 241, 441. John Wiley, New York (1963).
4. M. C. Jones, Mechanical properties of stacks under compression and vibration, M.Sc. Thesis, University of Wales (1965).
5. E. H. W. Schmidt and E. Jung, Measurement of the thermal contact resistance from stainless steel to liquid sodium, in *Modern Developments in Heat Transfer*, edited by W. Ibele, 251–263. Academic Press, New York (1963).
6. J. J. Bernard, La resistance thermique de joints, AGARD Report 212 (1958).
7. R. P. Mikesell and R. D. Scott, Heat conduction through insulating supports in very low temperature equipment, *J. Res. Natn. Bur. Stand.* **57**, 371–378 (1956).
8. S. D. Probert, T. Thomas and D. Warman, Cryostat for measurement of heat conduction under mechanical loads, *J. Scient. Instrum.* **41**, 88–91 (1964).
9. S. D. Probert, C. B. Thomas and T. Thomas, A high-stability current source, *Lab. Pract.* 458–459 (1965).
10. P. M. Lang, Calculating heat transfer across small gas-filled gaps, *Nucleonics* **20**, 62 (1962).
11. R. G. S. Skipper and K. J. Wootton, Thermal resistance between uranium and can, *2nd Int. Conf. Peaceful Uses Atom. Energy* **7**, 684–690 (1958).
12. Yu. P. Shlykov and Ye. A. Ganin, Thermal resistance of metallic contacts, *Int. J. Heat Mass Transfer* **7**, 921–929 (1964).
13. T. N. Cetinkale and M. Fishenden, Thermal conductance of metal surfaces in contact, *Proceedings of the International Conference on Heat Transfer*, p. 271. Instn Mech. Engrs, London (1951).
14. O. A. Saunders, Notes on some radiation heat transfer formulae, *Proc. Phys. Soc. Lond.* **41**, 569 (1929).
15. S. D. Probert and T. Thomas, Heat leaks through rarefied gases, *J. Scient. Instrum.* **41**, 182–183 (1964).
16. C. N. Patterson, *Molecular Flow of Gases*, p. 191. John Wiley, New York (1956).
17. L. C. Laming, Thermal conductance of machined metal contacts, *Proceedings of the International Conference on Developments in Heat Transfer*, Vol. 1, p. 65. Boulder, Colorado (1961).
18. R. Holm, *Electric Contacts Handbook*, 3rd edn., p. 62. Springer, Berlin (1958).
19. J. A. Greenwood and J. D. P. Williamson, The contact of nominally flat surfaces, Burndy Corp. Research Report 15 (1964).
20. R. W. Vance and W. M. Duke, *Applied Cryogenic Engineering*, p. 165. John Wiley, New York (1962).

Résumé—Afin d'obtenir un isolant thermique pour les températures cryogéniques, qui possède une résistance mécanique, on a mesuré dans le vide les variations en fonction de la charge appliquée des conductances thermiques d'empilements de feuilles minces d'acier inoxydable, d'acier à outils, d'acier pour lames de rasoir, de résine phénolique et de laiton à la température ambiante et à celle de l'azote liquide. On montre que chaque conductance se décompose en une composante constante, due aux pertes de chaleur radiales par conduction et rayonnement et une autre proportionnelle à la charge à une puissance comprise entre 0,5 et 1. Le dernière composante est inversement proportionnelle au nombre d'interfaces et on discute brièvement ce résultat du point de vue des théories existances. Les propriétés mécaniques et thermiques des colonnes multicouches sont comparables à celles des isolants existants, bien que quelques inconvénients soient possibles.

Zusammenfassung—In einem Versuch, einen mechanisch festen, thermischen Isolator zum Gebrauch bei kryogenen Temperaturen herzustellen, wurden die Änderungen der Wärmeleitfähigkeit von Stapeln dünner Lagen aus Stainless Steel, Werkzeugstahl, Rasierklingenstahl, Phenolschichten und Messing unter aufgebrachter Last im Vakuum bei Zimmertemperatur und bei der Temperatur des flüssigen Stickstoffs gemessen. Es zeigt sich, dass jede Leitfähigkeit aus zwei Komponenten besteht: einem konstanten Anteil infolge radialer Wärmeverluste durch Leitung und Strahlung und einem zweiten, der einer Potenz zwischen 0,5 und 1 der aufgebrachten Last proportional ist. Die letztere Komponente verändert sich umgekehrt wie die Zahl der Trennschichten; sie wird kurz nach Gesichtspunkten bestehender Theorien diskutiert. Die mechanischen und thermischen Eigenschaften der Vielschichtensäulen lassen sich gut mit jenen bestehender Isolatoren vergleichen, doch sind einige mögliche Nachteile in Betracht gezogen.

Аннотация—С целью создания механически прочного теплового изолятора для использования при криогенных температурах проведены исследования влияния нагрузок на теплопроводность для большого количества материалов в виде тонких слоев (нержавеющей стали, инструментальной стали, стали для бритвенных лезвий, фенола и бронзы) в вакууме при комнатной температуре и температуре жидкого азота. Показано, что в каждом случае эффективная теплопроводность слагается из двух составляющих: одна—постоянная, обусловленная утечкой тепла теплопроводностью и излучением, другая пропорциональная нагрузке в степени от 0,5 до 1. Этот последний компонент, который, как найдено, обратно пропорционален числу поверхностей раздела, кратко обсуждается с точки зрения существующих теорий. Показано, что многослойная колонна обладает хорошими механическими и термическими свойствами по сравнению с известными изоляторами. Рассмотрены некоторые недостатки таких материалов.